**Genome-Wide Screening and Physiological Responses of *Saccharomyces cerevisiae* to the Volatile Organic Compound 1-octen-3-ol**

by

David C. Pu

A thesis submitted to the

Graduate School-New Brunswick

Rutgers, The State University of New Jersey

in partial fulfillment of the requirements

for the degree of

Master of Science

Graduate Program in Plant Biology

written under the direction of

Dr. Joan W. Bennett

and approved by

_____

_____

_____

New Brunswick, New Jersey

May, 2012

## ABSTRACT OF THE THESIS

Genome-Wide Screening and Physiological Responses of *Saccharomyces cerevisiae* to the Volatile Organic Compound 1-octen-3-ol

By David C. Pu

Thesis Director:

Dr. Joan W. Bennett

A major fungal volatile organic compound (VOC) called 1-octen-3-ol or "mushroom alcohol," is produced by most fungal species and is responsible for much of their characteristic musty odor. We believe that fungal VOCs are serving as chemical compounds that signal within a single organism or signal within members of a single species. Also, fungal VOCs may cause "sick building syndrome" (SBS). In this study, we used *Saccharomyces cerevisiae* as a model for understanding 1-octen-3-ol toxicity on a genome-wide level. A yeast growth assay using solid media prepared in plates sealed with Parafilm was developed. Conditions were identified which permitted reproducible yeast growth measurements when cultures were exposed to 1-octen-3-ol, a challenge due to the volatile nature of the compound. At 48 hours, 300 ppm of 1-octen-3-ol was found to completely inhibit growth of BY4741, a wild type strain. To identify genes and pathways involved in 1-octen-3-ol resistance, we carried out a high-throughput viability assay using the non-essential yeast knockout (KO) library. Of the ~ 4976 strains, we found that 92 (1.8%) showed resistance to 300 ppm of 1-octen-3-ol of which 21 (22.8%) are related to endosome transport. More specifically, 1-octen-3-ol is very likely to inhibit cell grow by the ubiquitin-dependent protein catabolic process via the multivesicular body sorting pathway.

## ACKNOWLEDGMENTS

First and foremost, I would like to express my gratitude to my thesis advisor Professor Joan W. Bennett, without her extensive knowledge, patience and support, this project would not have been possible.

I also want to thank Professor Nilgun Tumer, Professor James White, and Dr. John McLaughlin for serving on my thesis committee and reviewing my dissertation in a professional and objective manner. Without their guidance and great suggestions, this project would not have been completed as efficiently as it was. Also, thanks for Professor Tumer's and Dr. McLaughlin's collaboration; they provided access to the yeast knockout (KO) library and screening tools in order to complete this project.

I also would like to thank fellow graduate students, lab members and colleagues. Thanks for being around when I most needed you. I especially thank Mohamed Anwar Bin-Umer and Dr. Michael Pierce for helpful technical support and discussions while I was doing the project.

I would also like to thank my family, especially my mom, Haiyen Pu, and sister, Jenny Pu. When I went home late, mom always had the dinner ready for me and told me to sleep early. Also, every time I called my sister, she always gave me great encouragement and told me to focus and finish strong for my graduate school life.

I would finally like to thank my friends, Wen-min Su, Huei-Ru Liao, Fang-Yu Lin, I-Hua Chen, and Shih-Hsien Yang. Every time I meet a problem in my research, they always encourage me and stay up with me in the library to finish my report and studies.

## TABLE OF CONTENTS

## LIST OF TABLES

## LIST OF FIGURES

# 1. INTRODUCTION AND BACKROUND

## 1.1 Fungal volatile organic compound (VOC) – 1-octen-3-ol

The overall goal of screening the yeast knockout library was to understand how 1-octen-3-ol affects cell physiology at the molecular level and on a genome-wide scale. This major fungal VOC, also called "mushroom alcohol", is produced by many fungal species (Kaminski & Wasowicz, 1974; Cole & Schweikert, 2003; Chiron & Michelot, 2005; Combet et al, 2006). The mushroom like odor of 1-octen-3-ol is recognized at 10 $\mu g/m^3$ while the musty odor of 2-octen-1-ol is recognized at 16 $\mu g/m^3$**.** Several other C-8 compounds contribute to these odor perceptions. Studies have shown that moldy odors were recognized at concentrations greater than 0.035 $\mu g/m^3$ (Wilkins & Larsen, 1995). Low levels of 1-octen-3-ol gives toxicity in two genetic models - *Drosophila melanogaster* (Inamdar et al, 2010) and *Arabidopsis thaliana* (Splivallo, 2007) as well as in human embryonic stem cells (Inamdar et al, 2012). *Saccharomyces cerevisiae* offers another excellent eukaryotic model system. Yeast cultures are quick and easy to grow and about 20 percent of human disease genes have counterparts in yeast (Pommerville, 2009). When a well-established human disease gene is expressed in yeast, it successfully complements a mutation abolishing the function of its yeast ortholog. For example, expression in *S. cerevisiae* of a mammalian RAS protein (one of several paralogs) results in restoration of viability to a double-mutant strain defective in both of the paralogous yeast RAS genes (Dolinski & Botstein, 2007). Also, with the benefit of the yeast knockout library and high-throughput screening tools, genes that contribute to the sensitivity or resistance to drugs and other chemicals can be rapidly identified to provide clues about the mechanism of activity. The *Saccharomyces* genome database (SGD)

(http://www.yeastgenome.org/) provides an extensive database about the vast majority of yeast genes. Furthermore, the identification of targets may provide methods to study the relationship between VOC exposure and "mold related illness."

### 1.2 Yeast knockout library

Yeast genome haploid deletion library from the mating type MAT**a** was purchased from Open Biosystems (https://www.openbiosystems.com/). One benefit of using this set of yeast deletion strains for functional profiling is that one can gather much information about human gene function by analogy (Dolinski & Botstein, 2007). Also, one can identify each strain which allows phenotypic analysis to be performed on a genome-wide scale.

The yeast knock out strains were originally created systematically using a PCR-based strategy (Wach, 1994). There were two sequential PCR reactions. The first sequential PRC reaction incorporated the appropriate tags and conferred the antibiotic resistance gene. The second sequential PRC reaction incorporated the mitotic recombination sites. Then, each open reading frame **(**ORF) was replaced with a KanMX cassette using homologous recombination. This method allowed for greater than 95% of the ORFs to be knocked-out. Each cassette contains a unique 20 base pair nucleotide sequence of DNA known as a "molecular barcode" allowing for parallel analysis. Also incorporated is a common set of flanking DNA tag sequences allowing amplification of the unique tags (Figure 1).

Evidence for the functional role of a gene can be obtained by analysis of the phenotypic changes exhibited by each mutant strain under a given condition. While this type of analysis has been performed in the past using traditional genetic screens or random mutagenesis, the yeast knock out strains offer advantages over both of

these methods. One advantage is that the phenotypes of the yeast mutant strains reflect a complete loss of function of the given gene. Furthermore, in contrast to traditional screening, the gene identification is known a *priori*, thereby removing the time-consuming task of determining the responsible gene (Giaever, 2002)

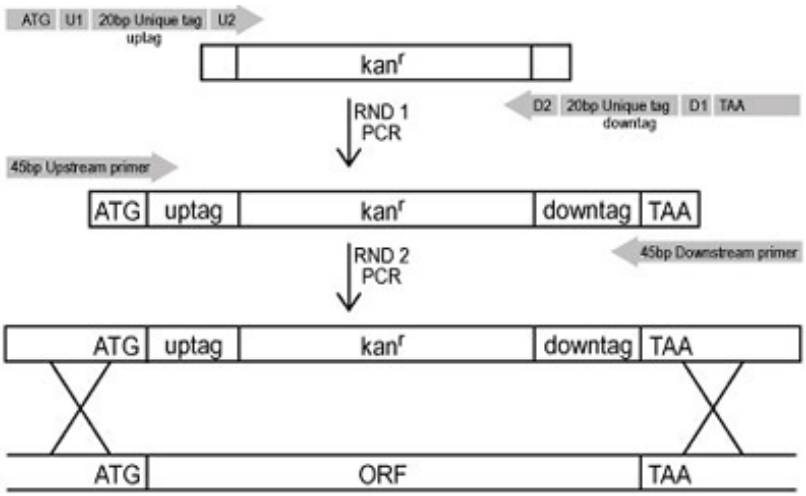


**Figure 1. Gene Knock-out Diagram** (Thermo Scientific)

### 1.3 Yeast gene nomenclature conventions

The yeast genes in the yeast knockout library are given by their systematic names. The Systematic Name of the stain is the name generated by the systematic sequencing project, or conferred later according to the appropriate guidelines for systematic nomenclature for that type of new feature or gene. The official Gene Name of an *S. cerevisiae* gene is referred to as the Standard Name on an SGD locus page, and generally becomes the standard name based on its publication in a peer-reviewed paper describing characterization of that gene (http://www.yeastgenome.org/help/community/nomenclature-conventions) (SGD Project). For the genes we screened in this study, most are named by nuclear encoded open reading frames (ORFs). For example, gene YAL001C, the systematic

names begin with the letter 'Y'; the second letter corresponds to the chromosome number (given in Roman numerals), e.g. chr I is 'A', chr VIII is 'H'; the third letter is either 'L' or 'R' for left or right of the centromere. Next is a three digit number indicating the order of the ORFs on one arm of a chromosome starting from the centromere. Finally, there is an additional letter, either 'W' or 'C' for Watson (the strand with 5' end at the left telomere) and Crick (the complement strand, 5' end is at the right telomere). The gene names in *S. cerevisiae* are generally three letters followed by a number. For example COX2 or CDC28, are names conferred to a gene by an individual researcher. Names may be conferred on the basis of genetic as well as biochemical or molecular characterization of the gene. Thus, gene names are conferred on any type of gene or feature that can be characterized genetically. Most genes having gene names are ORFs, but tRNAs and other non-protein coding RNAs have also received gene names. In addition, there are named genes in the *Saccharomyces* Genome Database (SGD) that have not yet been mapped to a physical location on the chromosome. The official gene name of an *S. cerevisiae* gene is referred to as the standard name on an SGD locus page, and generally becomes the standard name based on its publication in a peer-reviewed paper describing characterization of that gene (http://www.yeastgenome.org/help/community/nomenclature-conventions) (SGD Project). The biggest difference between the systematic name and gene name is that systematic name gives very specific gene information when people use the SGD data base to search for it. However, gene names may or may not include many similar systematic genes.

**1.4 Reactive Oxygen Species (ROS)**

From our earlier studies, we learned that 1-octen-3ol would cause reactive oxygen species (ROS) generation inside yeast cell and affect growth. From our interpretation, the ROS may be caused by the accumulation of the undegraded proteins due to the mislabeled ubiqutination from 1-octen-3-ol. Reactive oxygen species are constantly generated under normal conditions as a consequence of aerobic respiration. Free radicals and other "reactive oxygen (ROS)/nitrogen/chlorine species" are believed to contribute to the development of several age-related diseases such as Alzheimer's disease (Halliwell, 2001; Butterfield, 2002). Diseases such as cancer, atherosclerosis, diabetes, and other neurodegenerative diseases are also found to have an association with ROS (Hagen, 1994; Chowienczyk, 2000; Parthasarathy, 2000). In yeast, cells without mitochondria grow at a slower rate than those with mitochondria due to no help of alleviate ROS stress (Grant, 1997). In our experiments, the yeast cells without mitochondria (BY4743-rho$^{0}$) exposed to 1-octen-3-ol grew worse than the ones with mitochondria (BY4743-rho$^{+}$) (Figure2). We have used 2',7'-dichlorofluorescein diacetate (DCFH-DA) stain and flow cytometry to address the significance of ROS levels by the quantitative output from the flow cytomertry.

DCFH-DA is a cell permeable and non-fluorescent precursor of 2′,7′-dichlorofluorescin (DCF). It is extremely sensitive to changes in the redox state of cell and can be used to follow changes in ROS over time. It is currently one of the most widely used techniques for directly measuring the redox state of a cell. Inside the cell, intracellular esterases cleave DCFH-DA at the two ester bonds, producing a relatively polar and cell membrane-impermeable product, $H_2$DCF. This non-

fluorescent molecule accumulates intracellularly and subsequent oxidation yields the highly fluorescent product DCF (Eruslanov, 2010) (Figure 3).

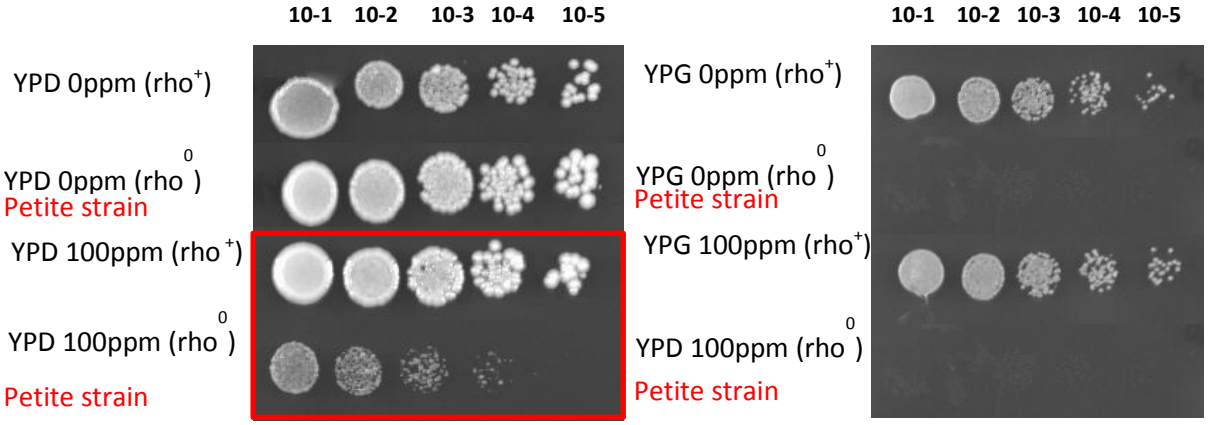


**Figure 2. Effects of 1-octen-3-ol on yeast (rho$^{+}$ and rho$^{0}$) with YPD and YPG medium**
In YPD (yeast peptone dextrose) medium, at 100 ppm, the strain with mitochondria (rho$^{+}$) grows similarly to the petie (rho$^{0}$) when no 1-octen-3-ol is added. However, the petite strain (rho$^{0}$) grows less than the control at 100 ppm (indicated in the red rectangle).

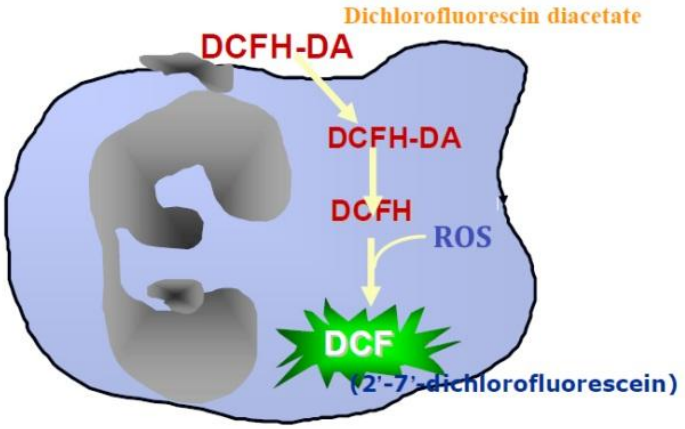


**Figure 3. The mechanism of DCFDA** (Lin et al, 2007)**.**

## 2. MATERIAL AND METHODS

### 2.1 Effect of 1-Octen-3-ol tested on yeast

Wild type yeast, BY4741, was first grown in Yeast Peptone Dextrose (YPD) liquid media overnight, which contains contains 1% Bacto yeast extract (Fisher Scientific), 2% Bacto peptone (Fisher Scientific). Then the yeast strain was serially diluted to five different concentrations – $10^{-1}$, $10^{-2}$, $10^{-3}$, $10^{-4}$, and $10^{-5}$ – and then spotted on six YPD agar petri plates. Petri plates contained different concentration of 1-octen-3-ol (Sigma-Aldrich): 0 ppm, 10 ppm, 50 ppm, 100 ppm, 200 ppm, and 300 ppm. The plates were sealed with four layers of parafilm, placed into a burken glass jar (IKEA), and incubated for 48 hours without shaking.

### 2.2 Yeast genome-wide screen using the yeast knockout (KO) library

The entire non-essential yeast knockout (KO) library consists of about 4976 strains. The library was initially arrayed in 96 well plates but was consolidated further to the 384 well format using a RoToR HDA pinning robot (Singer Instrument Company, LTD). Omnitray plates (Nunc) for screening were prepared by adding 37.5 ml of yeast peptone dextrose (YPD) agar medium, which contains 1% Bacto yeast extract (Fisher Scientific), 2% Bacto peptone (Fisher Scientific), 2% Bacto argar (Sigma-Aldrich), the antibiotic G418 100µg/µl, and 2% dextrose, with the pH adjusted to 6.8. All the strains were pinned by the RoToR HDA and plates maintained aerobically at 30℃ in a static incubator for 2 days. Further, all the cultures were pinned again using RoToR HAD in the black 384-well Microtest™ Plate (BD Falcon) for cell dilution with 60 µl of YPD per well. After the dilution, all cells were again plated using the RoToR HDA, to pin on a total of 15 OmniTrays. The entire Yeast KO library was separated to 15 OmniTrays and we screened three

plates at a time. Each plate was represented by two duplicate treatments and one control plate. Each treatment plate contained six glass cover slips; four were placed evenly on the four corners of the plate lid and the other two cover slips were placed on the middle of top and bottom plate lid thus avoiding direct physical contact with the liquid phase of the volatile organic compound, 1-octen-3-ol, and the plate. All the treatments plates were exposed to 250 parts per million (ppm) of 1-octen-3-ol wrapped with four layers of Parafilm (VWR) and incubated with their control plates in the HiGro-incubator at 30℃ with shaking (250 rpm).

**2.3 Confirmation of the identified resistant YKOs by viability assay**

The confirmation of the resistance genes from the first screening was done by performing viability assays. The yeast resistance strains were serially diluted to five different concentrations – $10^{-1}$, $10^{-2}$, $10^{-3}$, $10^{-4}$, and $10^{-5}$ – and then spotted on 10 Omnitrays with duplication for each plate. All of the plates contained 300 ppm of 1-octen-3-ol (Sigma-Aldrich). The plates were further wrapped with four layers of Parafilm (VWR) and incubated with their control plates in the HiGro-incubator at 30℃ with shaking (250 rpm)

**2.4 Reactive Oxygen Species (ROS)**

Five mM DCFH-DA (Sigma) solution was made with 99% ethanol and stored at room temperature protected from the light. The yeast wild type strain, BY4741, was cultured in YPD agar petri plates in a stationary incubator for 48 hours. Treatment plates are using the same yeast screening technique above – two glass slides were placed on the cap of the petri plate and different concentration of 1-octen-3-ol was applied on the top of the glass slides. Plates were further sealed with four layers of parafilm and incubated in a shaking incubator at 30℃ for two hours. After two hours,

control and treatment cells (cell OD = 0.1) were placed in different eppendorf tubes with one mL of sterile water. 10 uL of 5 mM DCFH-DA solution was applied to both control and treatments tubes and covered with aluminum foil and grow in 30℃ shaking incubator for 20 minutes. The cells were further washed with sterile water and ready to read in flow cytomertry.

## 3. RESULTS

### 3.1 1-octen-3-ol yeast assay

In order to perform the screening, the sensitivity of yeast to 1-octen-3-ol was measured using viability assays. Wild type yeast strain, BY4741, was grown on YPD and then different concentrations of 1-octen-3-ol were tested– 0ppm, 50ppm, 100ppm, 200ppm, and 300ppm – by placing aliquots onto glass slides. 1-octen-3-ol comes in liquid form and becomes a volatile upon evaporation. The petri dishes were sealed with two layers of parafilm and stored in the Burken glass jar to prevent further evaporation and incubated in the 30 oC stationary incubator (Figure 4a). This set up gave us a broad range to determine the right concentration for screening. After two days of incubation, inhibition of cell growth due to 1-octen-3-ol is observed in the 100ppm treatment (Figure4b).

Figure 4a

Figure 4b

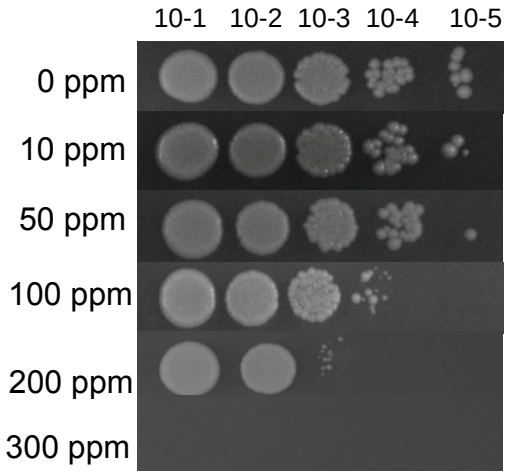


**Figure 4. Setup of petri dish in Burken jar and effect of 1-octen-3-ol on yeast.**
**Figure 4a.** A diagram of the petri dish placement inside the jar.
**Figure 4b.** The effect of 10, 50, 100, 200, and 300ppm 1-octen-3-ol on cell growth after 48 hours. Beginning at 100 ppm, 1-octen-3-ol is seen to inhibit yeast growth. As the toxin concentration is increased to 300 ppm, yeast growth becomes totally inhibited at 48 hours.

### 3.2 Yeast genome-wide screen by using yeast knockout (KO) library

The yeast genome-wide screening with the yeast knockout (YKO) library was performed using omnitrays. The omnitrays are necessary in order for the automatic pinning machine called RoToR HAD to print. Before using the automatic pinning robot, we first used a manual pinning tool to spot the wild type yeast strain, BY4741, to determine the parameters for the screening. The first omni-tray set up we tried was similar to the petri dish protocol. The plates spotted on the omnitrays with yeast (cell OD = 0.1) and then aliquots of 1-octen-3-ol on a glass slide were placed randomly in the plate. However, applying 1-octen-3-ol in only one spot did not provide uniform distribution of the volatile. Therefore, we divided the aliquot of 1-octen-3-ol four ways and observed yeast growth. Again, the results were not uniform because near the bottom of the plate edge, yeast cells were growing. These observations suggested that we should increase the number of glass slides to distribute the aliquots of 1-octen-3-ol. One explanation of why the cells grow better on the edges is because the plates were tilted when we placed them in the jar. This fungal VOC often absorbs water from the atmosphere under highly humid conditions (Cilek & Hallmon, 2008). Therefore, once 1-octen-3-ol absorbs water, it becomes heavier than atmospheric air causing the volatile to sink to a low level of the plate and this is the likely cause of the uneven growth phenomenon (Figure 5).

Figure 5a

Figure 5b

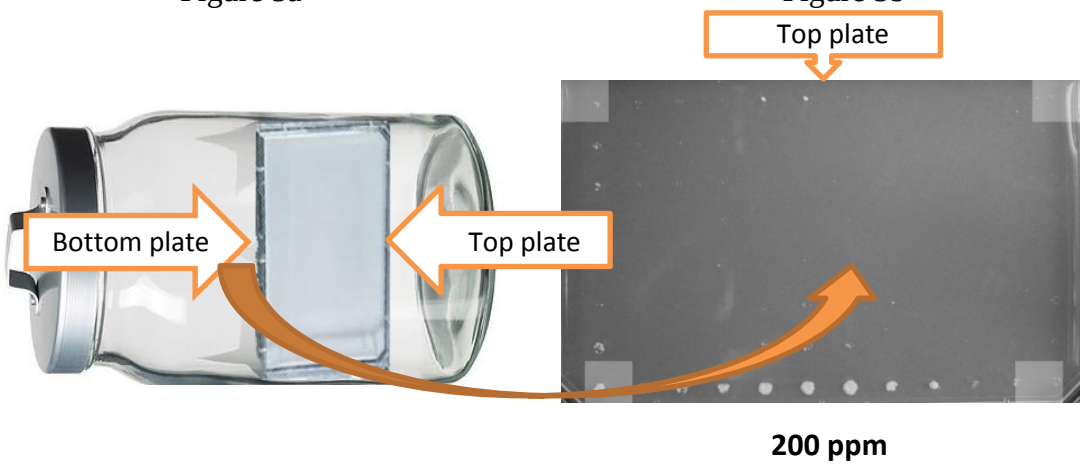


**Figure 5. Setup of omnitray in Burken jar**
Setup of omnitray in Burken jar with plate direction labeled (a) and
There is uneven cell growth toward the bottom and middle of the plate (b).

Finally, the number of glass slides was increased to six and the omnitrays were moved to a shaking incubator. The benefit of using a shaking incubator is to have the volatiles spread evenly in the test system thereby avoiding the inconsistency we saw with the tilted plates. However, the Burken jar glass bottle was not able to fit into the shaking incubator. We compensated by using more parafilm to prevent the leaking of 1-octen-3-ol, a shaking incubator, HiGro, to distribute volatile evenly in the plate, and rubber bands to keep the plates stable during shaking. Finally, this set up with six cover glass slides, four layers of parafilm, two thick rubber bands, 200 ppm of 1-octen-3-ol, and a 200 rpm shaking incubator satisfied our screening condition. However, when we used the robot to print, the cell optical density (OD) picked up by the robot cannot be adjusted as we did by using the manual pinning tool because the strains in the yeast KO library have different growth rates; some of strains grow faster than the other. Therefore, we increased the level of 1-octen-3-ol to 300 ppm to optimize the screen setup (Figure 6).

Figure 6a Figure 6b

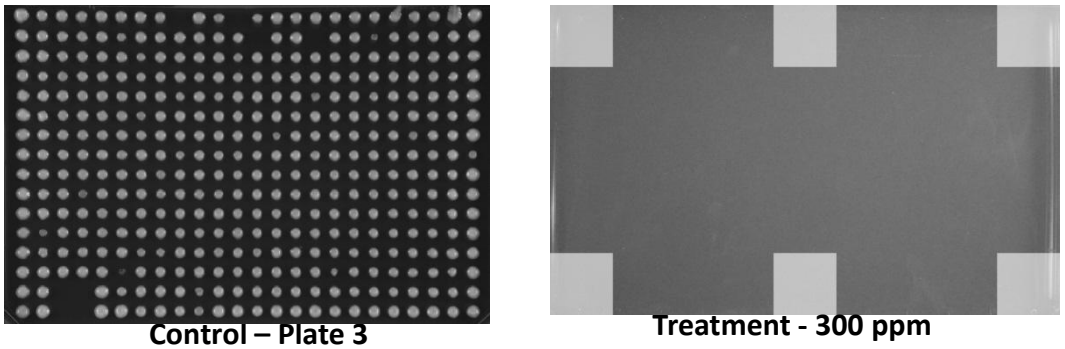


**Figure 6. The setup of omnitray with shaking and the even growth of yeast on 1-octen-3-ol.**
**Figure 6a.** Control plate of plate 3 in the Yeast knockout (YKO) library.
**Figure 6b.** At 300 ppm no cell growthwas observed in the presence of 1-octen-3-ol.

There are about 4976 strains in the YKO library, representing knockouts for all the non-essential genes in the YKO library. The library was consolidated into the 384 well format on 15 Omni trays. For each of the library plates, two replicates were made for each treatment and one replicate for the control. The entire library was screened twice. If one of the duplicated treatment plates failed to give identical results, that library plate was tested again. Strains were identified as presumably resistant when growth of a particular knockout strain was observed on both replicate plates in the presence of 300ppm 1-octen-3-ol. Figure 7 serves as an example of how the presumptive resistant strains were selected. The colonies with red circles are the resistant strains and the wells with green circles are the empty spot in the library plate.

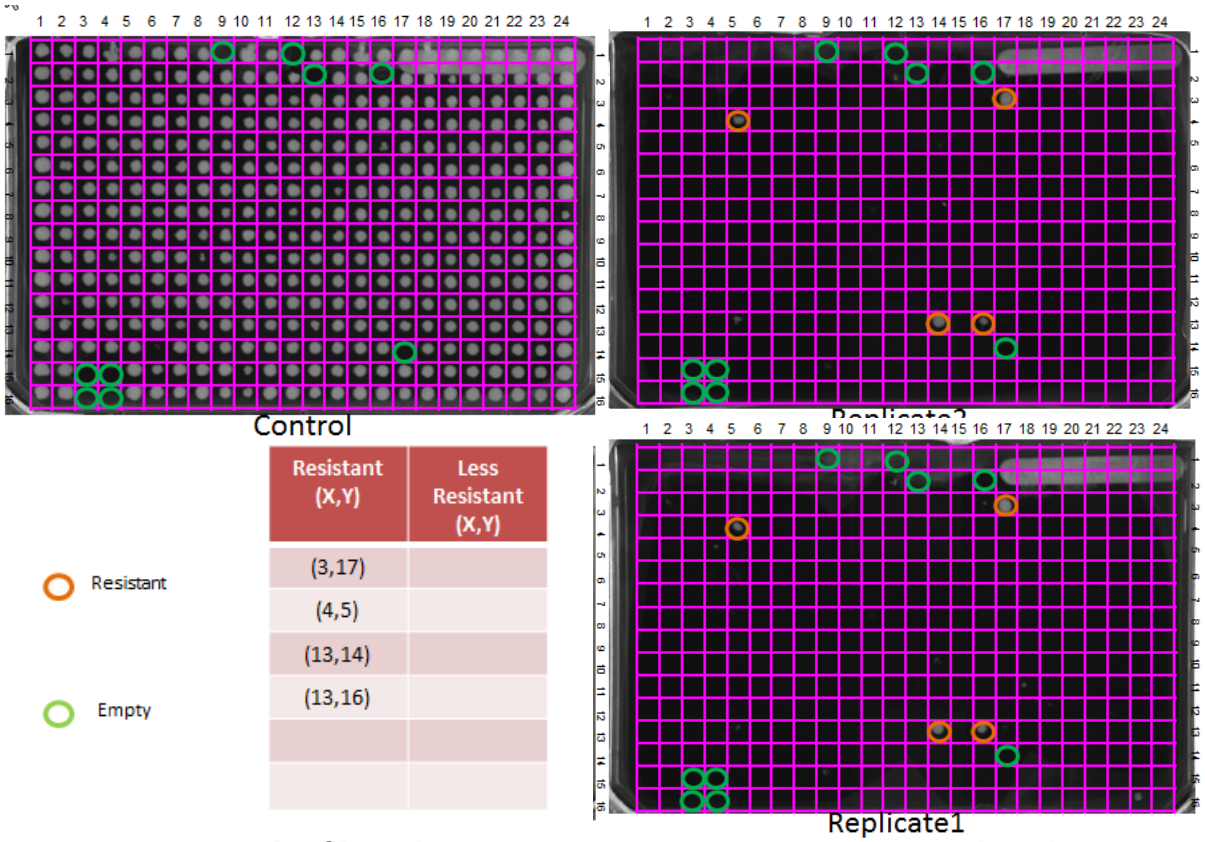


**Figure 7. An example of how the presumptive resistance strains were selected.** The green circle represents an empty spot in the library plate. The red circles show colony growth and represent the presumptive resistant strains. The table on the left bottom shows the location of the resistant strains on the matrix.

### 3.3 The resistant strains identified from the screening

Among the 4976 strains, we found 92 strains showing resistance to 1-octen-3-ol compared to the wild type stain, BY4741 and their conformation was performed by the viability assay (Figure 8). Twenty-one out of our 92 resistance genes are related to endosome transport based on gene ontology cluster analysis. A total of 77 genes in the database are grouped in the endosome transport category which accounts for 1.2% of the whole yeast genome (Table 1). It is striking that 22.8% of all strains showing resistance to 1-ocen-3-ol involve endosome transport. Moreover, since there are only a total of 77 genes involving endosome transport in the yeast genome, it is even more striking that 28 % of them are somehow related to the likely metabolism/transport of 1-octen-3-ol. In contrast, 18 out of 92 genes cluster in the protein targeting category and 15 out of 92 genes cluster in the proteolysis category. There are a total of 264 genes involved in protein targeting and 192 genes involved in proteolysis, giving only 6% and 16.3%, respectively.

**Figure 8. Confirmation of the identified resistant YKOs.** The following viability assays represent the confirmation of the 92 yeast resistance strains from the initial screen using the robot.

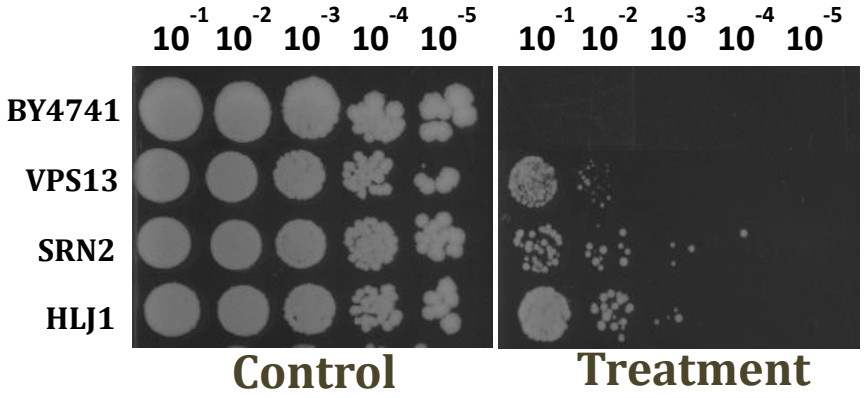

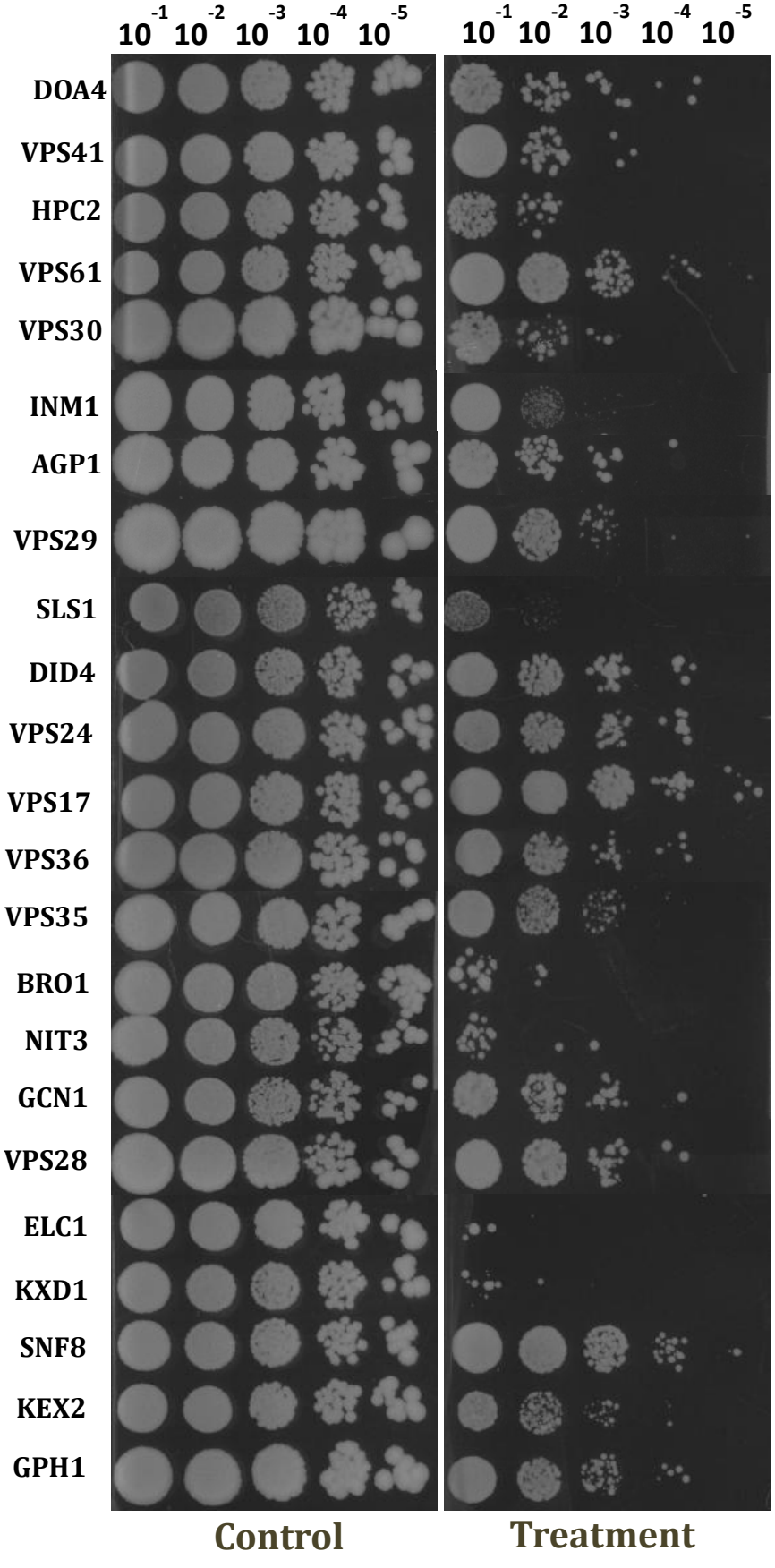
10-1 10-2 10-3 10-4 10-5
10-1 10-2 10-3 10-4 10-5
DOA4
VPS41
HPC2
VPS61
VPS30
INM1
AGP1
VPS29
SLS1
DID4
VPS24
VPS17
VPS36
VPS35
BRO1
NIT3
GCN1
VPS28
ELC1
KXD1
SNF8
KEX2
GPH1
Control
Treatment

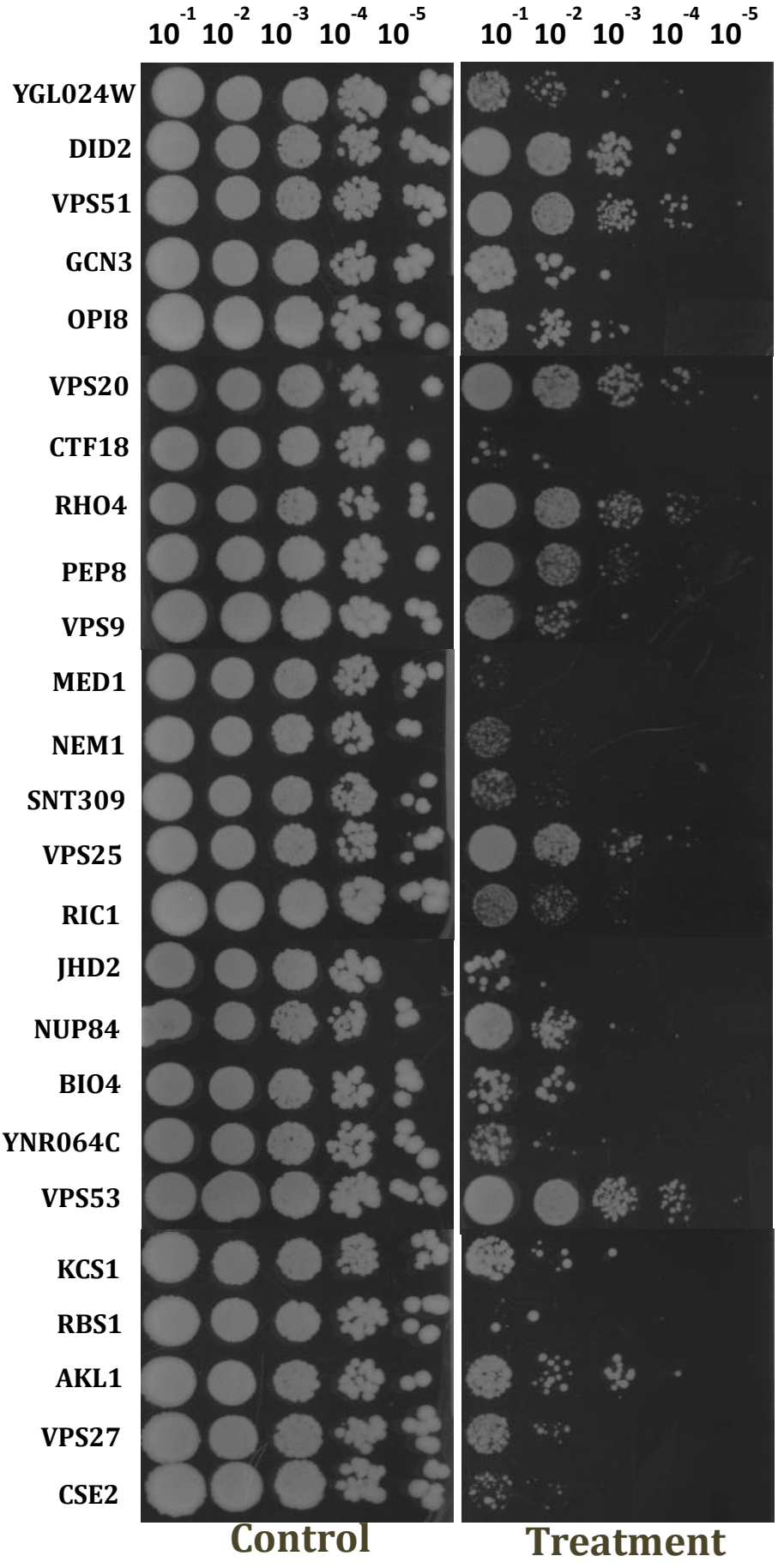
10-1 10-2 10-3 10-4 10-5
10-1 10-2 10-3 10-4 10-5
YGL024W
DID2
VPS51
GCN3
OPI8
VPS20
CTF18
RHO4
PEP8
VPS9
MED1
NEM1
SNT309
VPS25
RIC1
JHD2
NUP84
BIO4
YNR064C
VPS53
KCS1
RBS1
AKL1
VPS27
CSE2
Control
Treatment

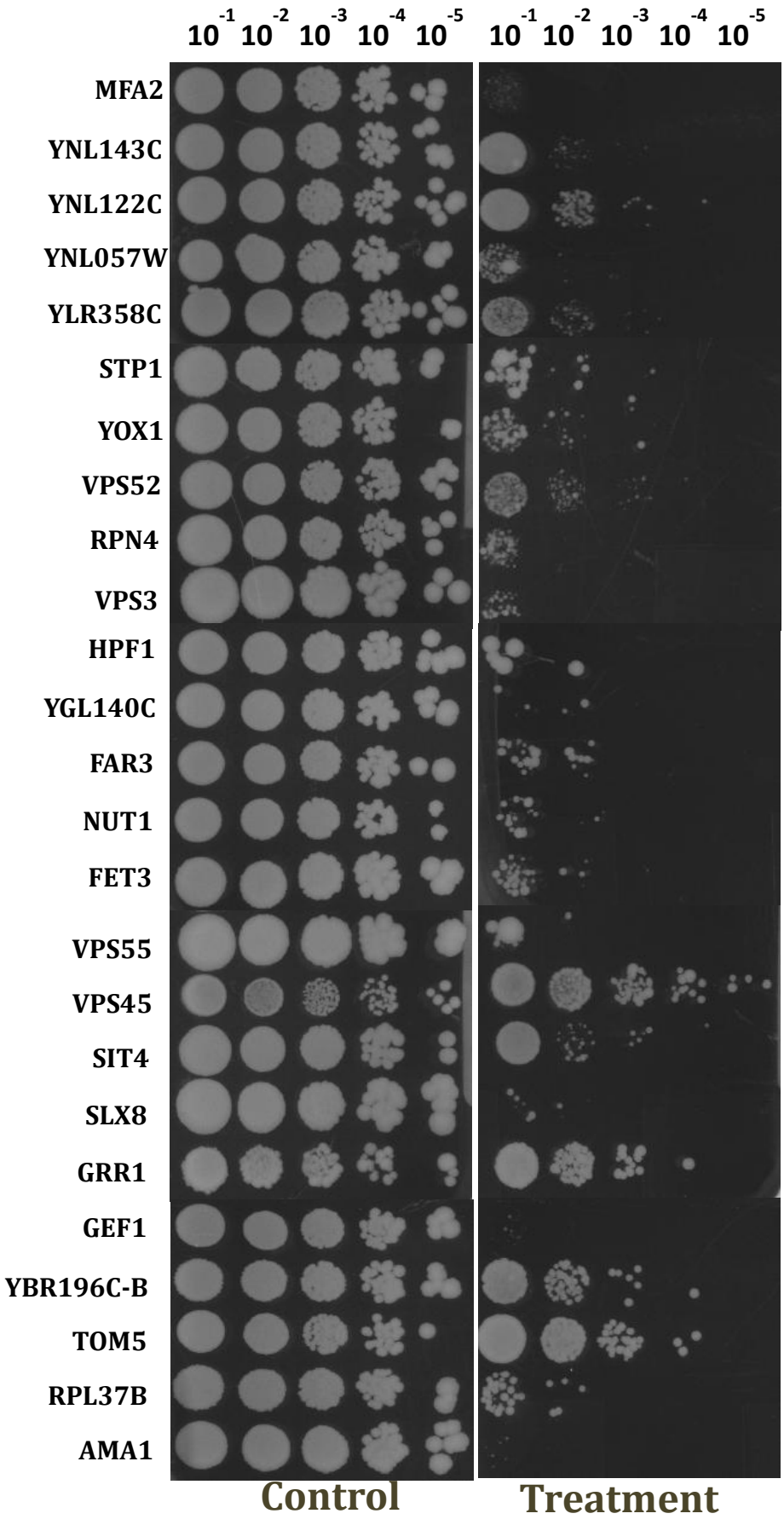
10-1 10-2 10-3 10-4 10-5
10-1 10-2 10-3 10-4 10-5
MFA2
YNL143C
YNL122C
YNL057W
YLR358C
STP1
YOX1
VPS52
RPN4
VPS3
HPF1
YGL140C
FAR3
NUT1
FET3
VPS55
VPS45
SIT4
SLX8
GRR1
GEF1
YBR196C-B
TOM5
RPL37B
AMA1
Control
Treatment

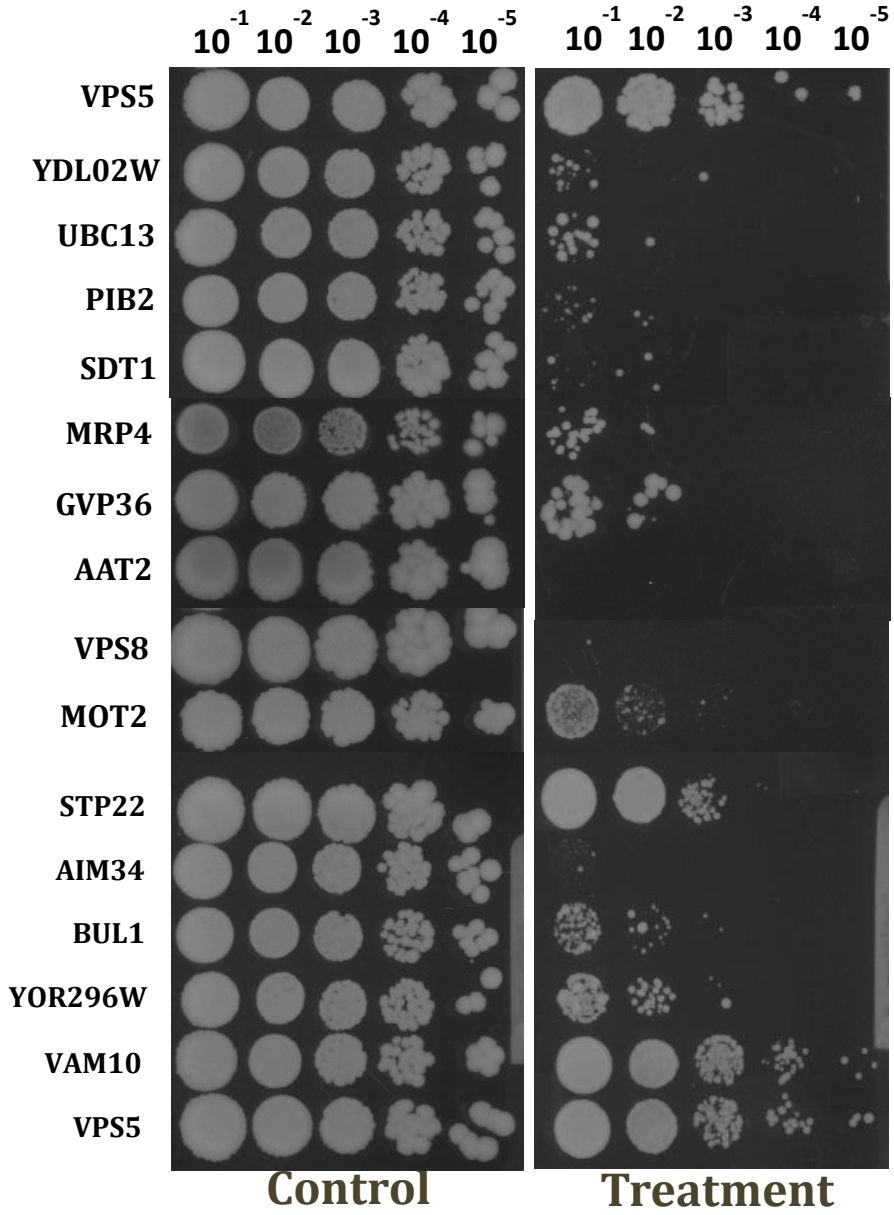


**Table 1. The number and frequency of the resistant genes grouped by biological process using Gene Ontology SLIM Mapper at SGD (SGD Project).**

| GO-Slim term | Cluster frequency | Genome frequency | Genes annotated to the term |
|---|---|---|---|
| endosome transport | 21 out of 92 genes, 22.8% | 77 of 6311 genes, 1.2% | BRO1, DID2, DID4, PEP8, RIC1, STP22, VPS13, VPS17, VPS20, VPS24, VPS27, VPS29, VPS30, VPS35, VPS45, VPS5, VPS51, VPS52, VPS53, VPS55, VPS8 |
| protein targeting | 18 out of 92 genes, 19.6% | 264 of 6311 genes, 4.2% | BRO1, DID2, NUP84, SNF8, SRN2, STP22, TOM5, VPS25, VPS27, VPS28, VPS3, VPS30, VPS36, VPS45, VPS51, VPS61, VPS8, VPS9 |

| | | | |
|---|---|---|---|
| **proteolysis involved in cellular protein catabolic processes** | 15 out of 92 genes, 16.3% | 192 of 6311 genes, 3.0% | BRO1, DID4, DOA4, ELC1, GRR1, HLJ1, SNF8, SRN2, STP22, VPS20, VPS24, VPS25, VPS28, VPS30, VPS36 |
| **biological process unknown** | 13 out of 92 genes, 14.1% | 1199 of 6311 genes, 19% | AIM34, KXD1, NIT3, OPI8, YBR196C-B, YDL026W, YGL024W, YGL140C, YLR358C, YNL057W, YNL122C, YNL143C, YOR296W |
| **response to chemical stimulus** | 11 out of 92 genes, 12% | 343 of 6311 genes, 5.4% | BRO1, FAR3, FET3, GRR1, MFA2, RPN4, SIT4, SNF8, VPS25, VPS36, YNR064C |

In the table above, the biological process ontology was used to classify our screening results by the SGD GO Slim Mapper tool. The top three categories (endosome transport, protein targeting, and proteolysis involved in cellular protein catabolic processes) have many overlapping genes. Therefore, the first, second, and third categories were merged to a category called the vacuolar protein-sorting (VPS) category, yielding a total of four categories which are VPS, biological process unknown, response to chemical stimulus and others. The "others" category represents biological processes which are not included in Table 2 such as transcription from RNA polymerase II promoter, response to DNA damage stimulus, protein modification by small protein conjugation or removal. In this re-organized chart, 37% of 1-octen-3-ol resistant genes are related to the VPS process, 14% are biological process unknown, 12% are "responds to chemical stimulus", 3% are overlapped between VPS and response to chemical stimulus, and 40% are in the "other" category. (Figure 9). In conclusion, the vacuolar protein sorting process is likely to be involved in 1-octen-3-ol transport or metabolism.

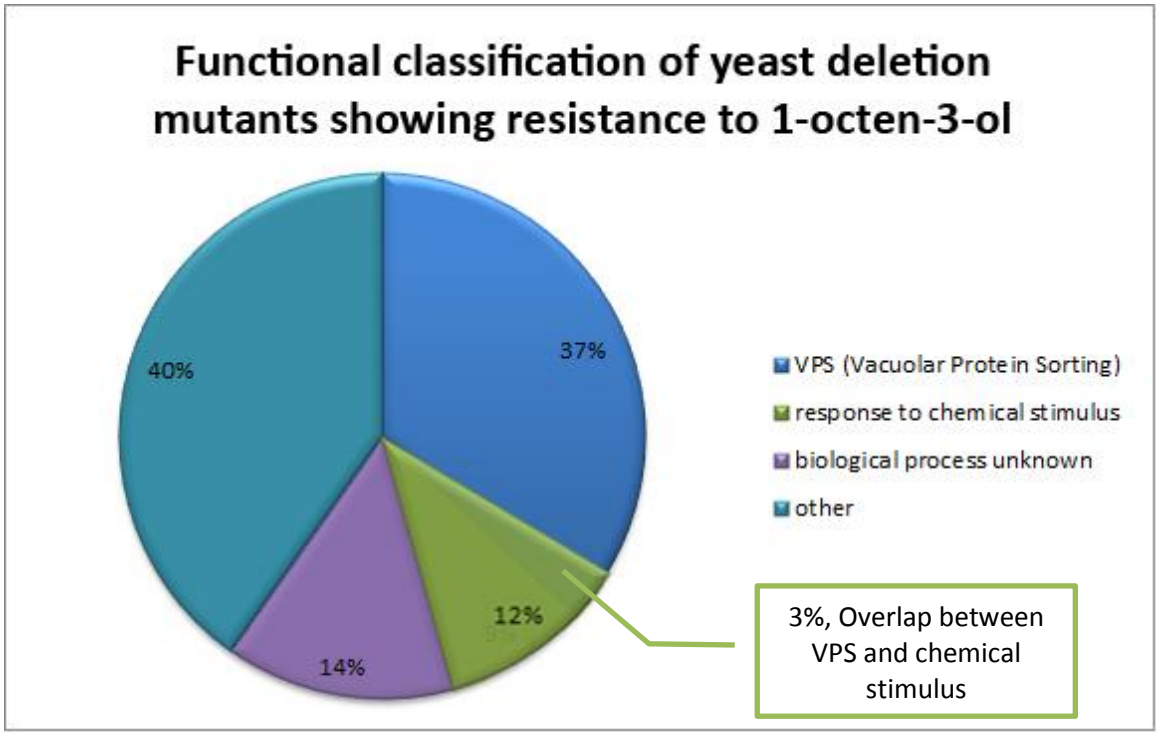


**Figure 9. Pie chart of functional classification of yeast deletion mutants showing resistance to 1-octen-3-ol.** The percentage of genes after combining the top three categories (endosome transport, protein targeting, and proteolysis involved in cellular protein catabolic process) is re-categorized to vacuolar protein sorting (VPS). Other categories include the genes in transcription from RNA polymerase II promoter, response to DNA damage stimulus, protein modification by small protein conjugation or removal. Interestingly, VPS is the major category of knockouts identified and confirmed in our screen.

Moreover, when we use components to categorize our genes, we found that 64 genes out of 92 resistance genes are in the cytoplasm, which accounts for about 70% of the resistance genes. Also, 34 out of 92 resistant genes are located in the membrane and 20 out of 92 resistance genes are in the nucleus. This re-categorization pie chart supports our previous hypothesis (based on biological process in SGD) because endosome transport happens in cytoplasm. Also, it is important to note that 13 out of 92 genes are located into mitochondrion. DOA4 is also associated with the mitochondrion (Table 2).

**Table 2. The number and portion of the 1-octen-3-ol resistant genes categorized with SLIM Mapper.**

| GO-Slim term | Cluster frequency | Genome frequency | Genes annotated to the term |
|---|---|---|---|
| cytoplasm | 64 out of 92 genes, 70% | 3819 of 6311 genes, 60.5% | AAT2, AIM34, AKL1, BIO4, BRO1, CTF18, DID2, DID4, DOA4, FAR3, GCN1, GCN3, GEF1, GPH1, GRR1, GVP36, HLJ1, INM1, JHD2, KCS1, KEX2, KXD1, MOT2, MRP4, NEM1, NIT3, NUT1, PEP8, PIB2, RBS1, RIC1, RPL37B, SIT4, SLS1, SNF8, SRN2, STP1, STP22, TOM5, UBC13, VAM10, VPS13, VPS17, VPS20, VPS24, VPS25, VPS27, VPS28, VPS29, VPS3, VPS30, VPS35, VPS36, VPS41, VPS45, VPS5, VPS51, VPS52, VPS53, VPS55, VPS8, VPS9, YNL122C, YOR296W |
| membrane | 34 out of 92 genes, 37% | 1446 of 6311 genes, 22.9% | AGP1, BUL1, DID4, FET3, GEF1, GVP36, HLJ1, NEM1, NUP84, PEP8, RHO4, RIC1, SLS1, SNF8, SRN2, STP1, STP22, TOM5, VAM10, VPS13, VPS17, VPS20, VPS24, VPS25, VPS28, VPS29, VPS35, VPS36, VPS41, VPS45, VPS5, VPS55, YGL024W, YGL140C |
| nucleus | 20 out of 92 genes, 22% | 2085 of 6311 genes, 33.0% | AMA1, CSE2, CTF18, ELC1, GRR1, HPC2, INM1, JHD2, MED1, MOT2, NUP84, NUT1, RIC1, RPN4, SIT4, SLX8, SNT309, STP1, UBC13, YOX1 |
| mitochondrion | 13 out of 92 genes, 14.1% | 1128 of 6311 genes, 17.9% | AIM34, CTF18, DOA4, GCN1, MRP4, NEM1, NIT3, NUT1, PIB2, SLS1, TOM5, VPS13, YNL122C |
| endomembrane system | 11 out of 92 genes, 12% | 360 of 6311 genes, 5.7% | GVP36, HLJ1, NEM1, NUP84, PEP8, RIC1, VPS17, VPS29, VPS35, VPS45, VPS5 |

Again, if we categorize the screen results using components by the SGD Slim mapper analysis tool, we can see that there are many overlapping genes between the cytoplasm and endomembrane. Therefore, we re-categorized these two categories into a category called cytoplasm endomembrane. Interestingly, there are many genes also overlapping between the new category, cytoplasm endomembrane, and other categories such as nucleus, mitochondrion, and especially membrane system.

Therefore, we decided to show the overlapping genes by using a Venn diagram-like figure so as to diagram the interaction between those genes. Five categories were used: cytoplasm endomembrane, (blue), nucleus (green), mitochondrion (purple), membrane (red), and others (milk white). The "Other" category includes the genes located in Golgi apparatus, cellular component unknown, plasma membrane, membrane fraction, ribosome, endoplasmic reticulum, cytoplasmic membrane-bounded vesicle, site of polarized growth, vacuole, cellular bud, mitochondrial envelope, extracellular region, chromosome, peroxisome, cell cortex, cytoskeleton, and cell wall (Figure 10). The overlapping area between the two colors represents the overlapping genes. For example, 16% (2% + 9% + 5%) of the genes are in the mitochondrion; 2% of the genes are overlapping genes between the mitochondrion and membrane (purple and red); and 5% are overlapping genes between the mitochondrion and cytoplasm (purple and blue). This composite figure indicates that while 1-octen-3-ol seems to affect many parts of the cell, the most affected parts involve the membrane and cytoplasm. Again, this supports the results we analyzed by using biological process in the SGD database because the endosome is a membrane-bound compartment in the cytoplasm and represents a large fraction of the identified resistant YKOs.

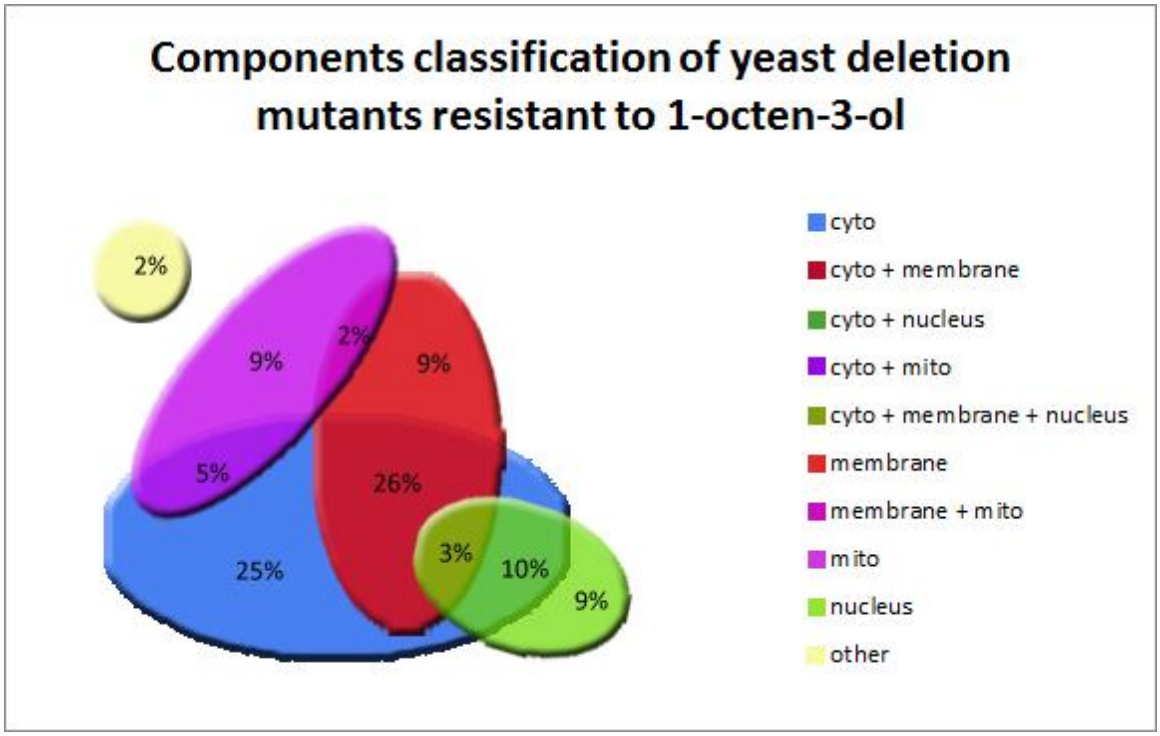


**Figure 10 Venn Diagram of cellular components classification of yeast deletion mutants resistant to 1-octen-3-ol.** This figure shows the percentage of genes in the cytoplasm (blue), mitochondrion (purple), membrane (red), and nucleus (green). Other (milk white) includes the genes in Golgi apparatus, cellular component unknown…etc. The percentages between two or three colors are the overlapping genes between the two or three components.

Furthermore, we also categorize those identified 92 strains by their resistance from the viability assay (Figure 7). Out of the 92 strains, there were two strains – ATT2 and VPS8 – which show no resistance to 1-octen-3-ol. The unit to calculate their resistance was colony forming units (CFU) per mL (Figure 11). We separate those strains to four categories - high resistance, resistant, moderate resistance, and low resistance. The cutoff point for high resistance, resistant, moderate resistance, and low resistance are $1x10^7$ CFU, $1x10^6$ CFU, $1x10^5$ CFU, and less than $1x10^5$ CFU respectively. In the end, we have 12 strains that fall into the category of high resistance. 29 strains fall in category of resistant. 23 strains fall in category of moderate resistance, and 25 strains fall in category of low resistance category ().

**Figure 11. Relative growth of BY4741 and the top 18 resistant mutants in the presence of 1-octen-3-ol.** Colony forming units (CFU) per mL of the top 18 resistance genes were plotted for level of resistance

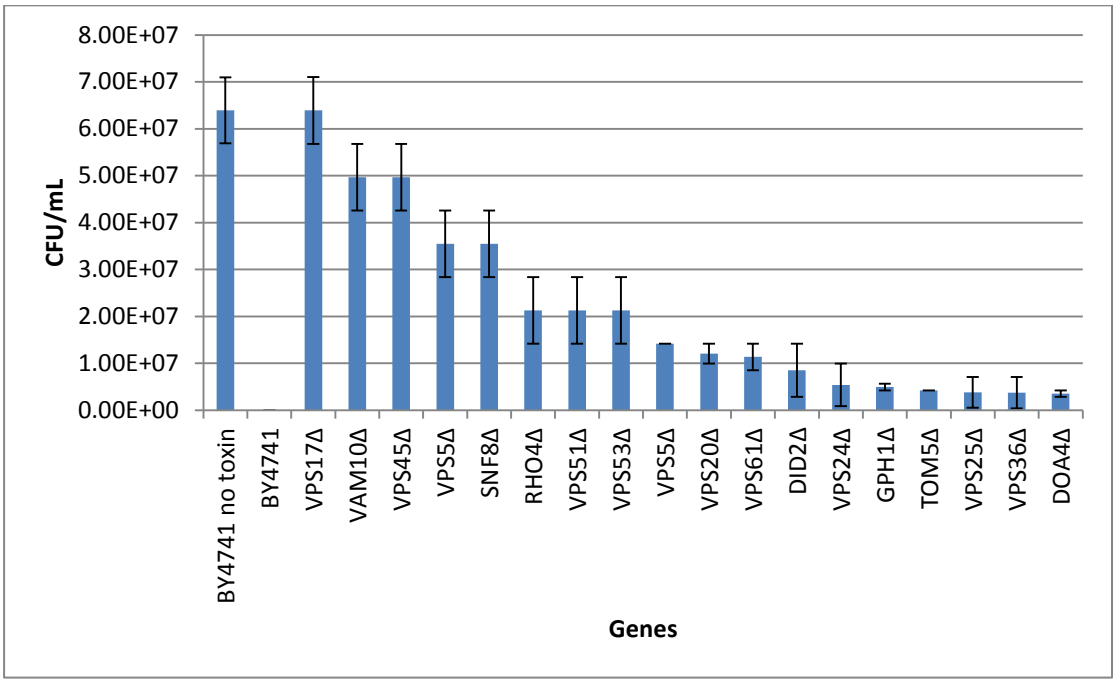


**Table3. Resistance strains categorization by the resistance level to 1-octen-3-ol.** Individual gene in the different categories and frequency.

| Level of resistance | Cluster frequency | Genes annotated to the term |
|---|---|---|
| high resistance | 11 out of 92 genes, 12% | VPS17, VAM10, VPS45, VPS5, SNF8, RHO4, VPS51, VPS53, VPS5, VPS20, VPS61 |
| resistant | 22 out of 92 genes, 23.9% | DID2, VPS24, GPH1, TOM5, VPS25, VPS36, DOA4, DID4, MRP4, YGL024W, VPS35, STP22, KEX2, AKL1, PEP8, VPS28, MOT2, VPS29, YNL122C, YBR196C-B, GRR1, SRN2 |
| moderate resistance | 26 out of 92 genes, 28.3% | HLJ1, BUL1, AGP1, NUP84, VPS52, GCN1, RIC1, SIT4, OPI8, YLR358C, INM1, VPS41, VPS30, YNL143C, YOR296W, YOX1, HPC2, VPS9, VPS27, STP1, VPS13, SLS1, GCN3, YNR064C, KCS1, FAR3 |
| low resistance | 33 out of 92 genes, 35.9% | CSE2, FET3, SNT309, YNL057W, BIO4, NIT3, JHD2, RBS1, NEM1, RPL37B, GVP36, PIB2, SDT1, BRO1, CTF18, HPF1, YGL140C, NUT1, AIM34, KXD1, MFA2, RPN4, VPS3, VPS55, SLX8, GEF1, YDL026W, UBC13, AMA1, ELC1, MED1, AAT2, VPS8 |

### 3.4 1-octen-3-ol inhibits yeast growth by ubiquitin-dependent protein catabolic processes via the multivesicular body sorting (MBS) pathway

In the total of 4976 strains, we identified 92 strains resistant to 1-octen-3-ol. The gene analysis tool in SGD Slim Mapper Tool (Gene Ontology clustering) and FunSpec ("Functional Specification") were used to identify lethal functions of resistant genes that are related to ubiquitin-dependent protein catabolic process via the multivesicular body sorting (MBS) pathway in the endosome (Table 4). Using the FunSpec classification tool, 10 genes from the screening result were categorized into the ubiquitin-dependent protein catabolic process via the MBS pathway in endosome from a total of 15 genes in this category represented in the database. After using the hypergeometric distribution, the p-value represents the probability that the intersection of given list with any given functional category occurs by chance which is less than $1 \times 10^{-14}$. This test is also including a Bonferroni-correction, a method used to address the problem of multiple comparisons. The Bonferroni-correction divides the p-value threshold that would be deemed significant for an individual test, by the number of tests conducted and thus accounts for spurious significance due to the multiple testing over the categories of a database.

**Table 4. Biological process results from the Funspec gene ontology cluster program.** The top most related categories from the data inputted into the program are listed. **K** is the number of genes from the input cluster in given category. **F** is number of genes total in a given category. The p-values represent the probability that the intersection of a given list with any given functional category occurs by chance. The Bonferroni-correction test was used to account for multiple comparisons. **Ubiquitin-dependent protein catabolic process via the multivesicular body sorting pathway** is the most significant category in this analysis.

| GO Biological Process (2062 catagories) | | | | |
|---|---|---|---|---|
| **Category** | p-value | In Category from Cluster | k | f |
| **ubiquitin-dependent protein catabolic process via the multivesicular body sorting pathway [GO:0043162]** | <1e-14 | STP22 DOA4 VPS25 DID4 VPS24 SRN2 VPS36 VPS20 SNF8 VPS28 | 10 | 17 |
| **retrograde transport, endosome to Golgi [GO:0042147]** | 1.465e-13 | VPS52 VPS29 VPS53 PEP8 VPS35 VPS51 RIC1 VPS5 VPS17 VPS30 | 10 | 26 |
| **protein retention in Golgi apparatus [GO:0045053]** | 8.504e-12 | PEP8 VPS35 DID4 VPS13 VPS36 VPS27 VPS5 | 7 | 11 |
| **protein targeting to vacuole [GO:0006623]** | 1.786e-11 | STP22 VPS3 VPS25 VPS51 DID2 SRN2 VPS36 VPS9 VPS27 SNF8 VPS28 | 11 | 53 |
| **late endosome to vacuole transport [GO:0045324]** | 2.601e-11 | VPS8 STP22 DID4 VPS24 DID2 VPS13 VPS20 VPS27 VPS30 | 9 | 29 |
| **protein transport [GO:0015031]** | 2.928e-11 | VPS8 STP22 NUP84 VPS41 VPS52 VPS29 VPS53 PEP8 VPS35 VPS25 DID4 VPS24 VPS51 DID2 VPS13 SRN2 VPS36 VPS20 VPS5 VPS17 SNF8 VPS28 VPS30 TOM5 | 24 | 412 |

**3.5 Reactive oxygen species (ROS) experiments**

In our study, we found that 1-octen-3-ol induced ROS generation. Yeast cells were incubated at 30$^{o}$C for two and half hours using a higher concentration of 1-octen-3-ol that was used for the screening because we found that timing is a critical aspect to ROS level. If we expose 1-octen-3-ol to the yeast for too long, we found very small or no changes in ROS levels based on the flow cytometric analysis. We may need to do a time course experiment in future. Within two and half hour exposure of 1-octen-3-ol at 900 ppm, there is not much ROS reaction based on flow cytomertry analysis. At 900 ppm, 1200 ppm, and 1500 ppm exposure to 1-octen-3-ol, first fluorescence detector (FL1) readings were 753, 2360, and 1155, respectively. For the 900 ppm treatment, almost no ROS generation was detectable, the ratio is only 1.16 (753/645) times the control level. Increasing the volatile treatment to 1200 ppm results in a higher ROS reaction compared to the non-treated control; the median FL1 reading is 3.5 (2360/645) times higher than the control. However, 1500 ppm only gives about 1.7 (1155.50/645) times greater than the control (Table 4). In the second experiment, we narrowed down the concentration of 1-octen-3-ol to approximately 1200 ppm. The results for 1200 ppm show a slightly lower ratio than previous results; however, it is still 3.4 (2206/645) times higher than the control and 1000 ppm is 1.9 (1233/646) greater than then control. At 1400 ppm, the ratio is 3.3 (2144/646) times greater than then control (Table 5). Despite the variability, we can conclude that 1-octen-3-ol is causing ROS generation; the patterns of change of ROS levels are the same for both experiments. There was not much reaction when cell were exposed to 900 ppm, the reaction suddenly increased at 1200 ppm and dropped again around 1400 ppm.

It appears that exposure to 1-octen-3-ol that has to reach certain level of concentration in order to stimulate ROS generation beyond the level observed in the non-volatile control treatments. The concentration and the exposure time are very critical for the compound to cause detectable ROS effect. The loss of ROS level may be due to the death (or induction of quiescence) of the yeast cells. It would be interesting to test ROS levels in mammalian cell cultures treated with 1-octen-3-ol.

**Table 5**. **Results of ROS level with two and half hours of 1-octen-3-ol treatment of wild type yeast, BY4741** (a)Results of ROS from the treatment 1-octen-3-ol in wild type yeast BY4741 following by control, positive control, 900 ppm, 1200 ppm, and 1500 ppm. There are 3.5 fold differences between the control and 1200ppm treatment. At 1500 ppm, ROS level starts to drop down. (b) Similar results are seen at 1000 ppm, 1200 ppm, and 1400 ppm. At 1200 ppm, the highest ROS reaction was observed. Also, at 1400 ppm, ROS level starts to drop again. First fluorescence detector (frequently called **FL1**).

**(a)**

| Plot 3: Multiple Samples | Count | Median FL1-A |
|---|---|---|
| A01 control : This Plot | 25,000 | 645 |
| A02 positive control : | 25,000 | 9,059.50 |
| A03 9ooppm : This Plot | 25,000 | 753 |
| A04 1200ppm : This Plot | 25,000 | 2,360.00 |
| A05 1500ppm : This Plot | 25,000 | 1,155.50 |

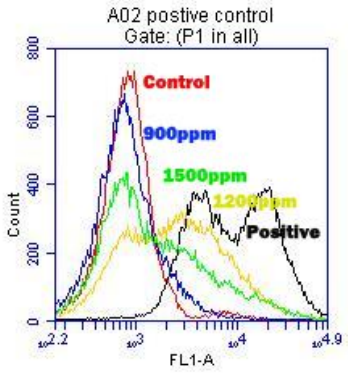


**(b)**

| Plot 4: Multiple Samples | Count | Median FL1-A |
|---|---|---|
| BY4741_Control : | 25,000 | 645 |
| BY4741_Positive_H2O2 | 25,000 | 3,151.00 |
| BY4741_1000-1 : | 25,000 | 1,233.00 |
| BY4741_1200-1 : | 25,000 | 2,206.00 |
| BY4741_1400-1 : | 25,000 | 2,144.00 |

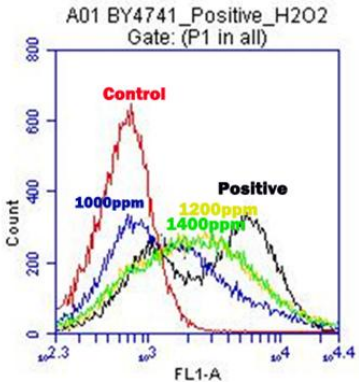

## 4. DISCUSSION

Protein degradation plays an important part in numerous cellular processes (Gottesman & Maurizi, 1992). It is a reversible post-translational modification of cellular proteins and is known to have central roles in regulating various cellular processes such as protein degradation, protein trafficking, cell-cycle regulation, DNA repair, apoptosis and signal transduction (Hershko & Ciechanover, 1998; Mukhopahyay & Riezman, 2007). In eukaryotic cells, proteins that must be rapidly destroyed are generally recognized and degraded by the ubiquitin system (Hochstrasser, 1996; Varshavsky, 1997). Ubiquitin is a highly conserved 76 amino acid protein that covalently attaches to the lysine residues of target proteins via its carboxyl-terminal glycine residue, forming an iso-peptide linkage in an ATP-dependent fashion. In general, the ubiquitination process is catalyzed by the sequential actions of three enzymes which are ubiquitin-activating enzyme (E1), ubiquitin-conjugating enzyme (E2), and an ubiquitin ligase (E3) (Kimura & Tanaka, 2010). Since ubiquitin itself contains seven lysines, it is able to attach repeatedly with other ubiquitins and allow the formation of polyubiquitin chains. With this special characteristic, ubiquitin can exist intracellularly either as a monomer, a substrate-conjugated polyubiquitin or monoubiquitin, or free (or unanchored) ubiquitin chains. There is a dynamic equilibrium among these three forms in the cell. Furthermore, the ubiquitination process can be reversed by deubiquitinating enzymes (Dubs) which are Ub-specific proteases. It is estimated that ~600 E3s and 100 Dubs exist in mammalian cells (Li et al, 2008).

In our screening study, we have found that the deletion of *DOA4* gene in yeast confers partial resistant to the fungal volatile organic compound (VOCs), 1-octen-3-ol. *DOA4* appears to play crucial roles in both ubiquitin-dependent proteolysis and

ubiquitin homeostasis (Papa et al, 1999). It is a well-studied Dubs and appears to function late in the ubiquitin-proteasome pathway by recycling ubiquitin from proteasome-targeted substrates (Amerik & Hochstrasser, 2000). When this gene is deleted, the resulting knockout strain shows accumulation of free ubiquitin chains or small ubiquitin species and reduction of monomeric ubiquitin (Papa & Hochstrasser, 1993). On the other hand, a gene called *RFU1* shows the opposite effect of *DOA4* when deleted. When Rfu1 is absent, there is accumulation of monomeric ubiquitin and reduced level of free ubiquitin chains. Furthermore, *RFU1* interacts with *DOA4* both *in vitro* and *in vivo* and recombinant Rfu1 inhibits the activity of *DOA4*, suggesting that *RFU1* is an inhibitor of *DOA4* (Kimura & Tanaka, 2009). In our screening, the yeast with lack of *RFU1* did not show any resistance in the presence of 1-octen-ol, suggesting that when yeast cell is treated with 1-octen-3-ol, it would be better for the ubiquitin to stay in the free ubiquitin chains. Interestingly, we also found that yeast grows in the presence of 1-octen-3-ol when the *BRO1* gene is deleted. Bro1p is required for the association of Doa4p with endosomes, where Doa4p catalyzes debuiquitination of multivesicular body (MVB) cargo proteins (Luhtala & Odorizzi, 2004). Doa4p is recruited to the endosome and its activity is stimulated by Bro1p, a class E vacuolar protein-sorting (Vps) protein (Luhtala & Odorizzi, 2004). When Bro1p is absent, Doa4p loses its localization in the endosome and shifts to cytoplasm, indicating that there is a balance of Doa4p and Bro1p (Luhtala & Odorizzi, 2004). In our studies, the Bro1 deletion strain shows resistance to 1-octen-3-ol. This suggests that *BRO1* is an important factor associated with 1-octen-3-ol toxicity. When *BRO1* is absent, most of the ubiquitin stays in the free ubiquitin chain phase. Bro1p is not able to bring Doa4p into the endosome and enhance monoubiquitin formation. Moreover, in the absence of *DOA4*, fewer MVB cargo proteins would be

deubiquitinatned. If those proteins do not get deuibiquitinated, they would be moved to MVB and be lysed by the lysosome, which suggests that 1-octen-3-ol disrupted the ubiquination process. The Rfu1p inhibits Doa4p changing free ubiquitin chain to monoubiquitin and Doa4p's deubiquitination activity. When *RFU1* is absent, ubiquitins are still getting changed to monoubiquitin and deubiquination is still going, hence, cells likely perform normally like the wild type stain when exposed to 1-octen-3-ol.

Moreover, besides *DOA4* and *BRO1*, other genes in the ubiquitin-dependent protein catabolic process via the multivesicular body sorting pathway category are subunits of endosomal sorting complex required for transport (ESCRT) complex. The formation of multivesicular bodies (MVBs) is a key stage in the delivery of cargo destined for degradation in the yeast vacuole or mammalian lysosome (Henne et al, 2011). The endosomal sorting complex required for transport-I (ESCRT-I) complex was characterized and shown to engage ubiquitinated cargo at the endosome and mediate its sorting into MVBs (Katzmann et al, 2001). The ESCRT-II and ESCRT-III complexes we identified as critical players in the delivery of ubiquitinated cargo to the yeast vacuole (Bsbst et al, 2002; Babst et al, 2002). Together, all these three papers established the ESCRT proteins as cargo sequestering and sorting machinery that can deform the endosomal-limiting membrane inward to generate MVBs. These studies were also significant in that they organized and assigned individual functions to the earlier identified "class E" vacuolar protein sorting (VPS) genes that, when knocked out in yeast, fail to deliver cargo to the vacuole and exhibit aberrant endosome morphology (Raymond et al, 1992). They also initiated work demonstrating that the ESCRTs comprise a pathway that recognize and sort ubiquitinated cargo through an exquisite division of labor.

Therefore, our interpretation is that 1-octen-3-ol affects ubiquitin labeled proteins. There are two main possibilities. First, those proteins which are supposed to get degraded, do not get degraded and accumulate inside the cell, causing cell arrest or death. Alternatively, many of the ubiqutinated proteins have been misallocated because of the disturbance caused by 1-octen-3-ol leading to cell arrest or death (Figure 12).

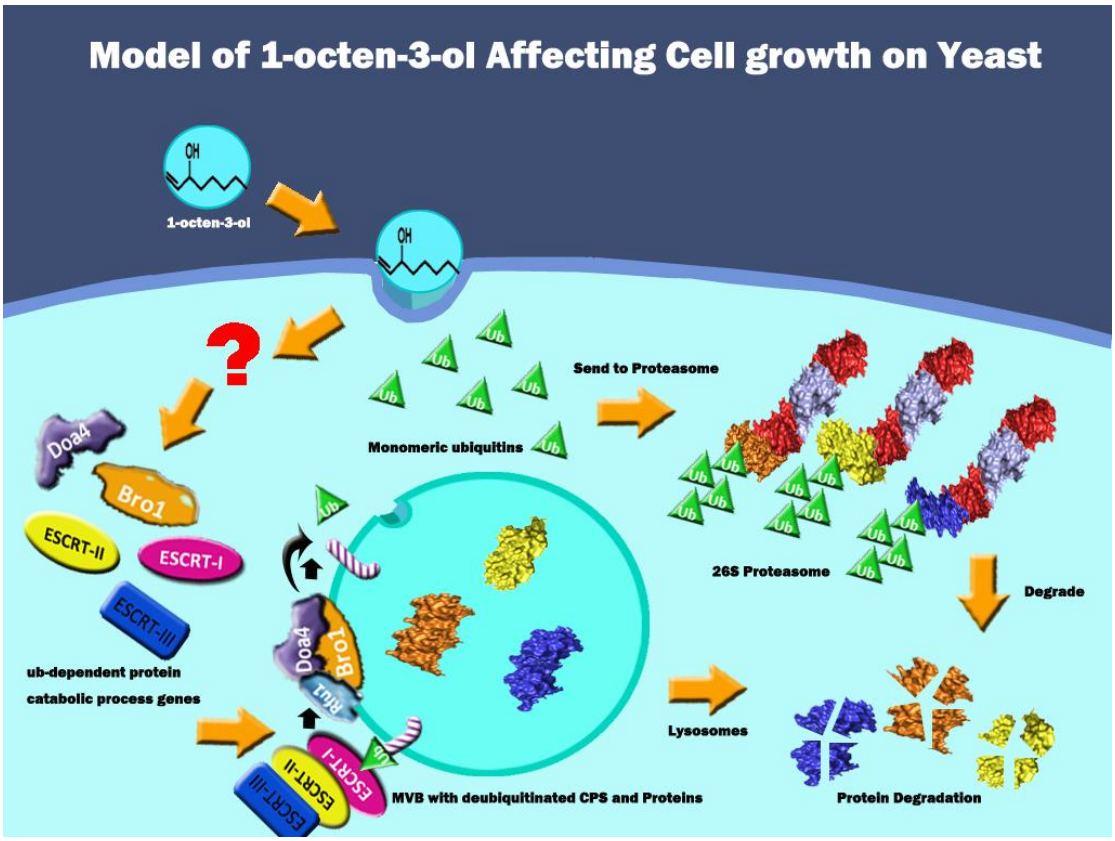


**Figure 12. Model of 1-octen-3-ol affecting cell growth on yeast.** From our screening, 1-octen-3-ol plays a role in disturbing the ubiquitined cargo process and further cause cell arrested or cell death. The resistance of DOA4 and BRO1 mutant also suggests us that the additional effect of cell arrest or cell death may cause by the imbalance of ubiquitin homeostasis.

Interestingly, numerous neurodegenerative conditions associated with mitochondria dysfunction are also known to have significant levels of proteasome inhibition, thus raising the possibility that proteasome inhibition may play a direct

role in inducing the observed mitochondrial dysfunction. In Sullivan et al, they have generated a clonal line of human SH-SY5Y cells that allows for the analysis of the cellular and molecular alterations that occur following low level proteasome inhibition. They found the ability of proteasome inhibition to directly alter multiple aspects of neural mitochondrial homeostasis and alter lysosomal-mediated degradation of mitochondria, demonstrating a possible role for proteasome inhibition serving as a direct mediator of neural mitochondrial dysfunction (Sullivan, et al., 2004). In our studies, reactive oxygen species (ROS) also occurred in yeast and when it is exposed to 1-octen-3-ol. Therefore, it is possible that 1-octen-3-ol disrupted the ubiquination process which alters mitochondrial homeostasis and further cause ROS generation.

Another interesting finding is that ubiquitin metabolism affects cellular responses to volatile anesthetics in yeast. *BUL1*, a ubiquitin ligase gene, appears to be involved in the ubiquitination pathway and this mutant was found to be resistant to all five volatile anesthetics tested they tested (Wolfe et al, 1999). Therefore, this work suggests that there are similarities in the mechanisms of action of a variety of volatile anesthetics in yeast and that ubiquitin metabolism affects response to those agents.

## 5. LITERATURE CITED

Amerik, A., & Hochstrasser, M. (2000). The Doa4 deubiquintinating enzyme is functionally linked to the vacuolar protein-sorting and endocytic pathways. *Molecular Biology of the Cell, 11*, 3365-3380.

Babst, M., Katzmann, D., Snyder, W., Wendland, B., & Emr, S. (2002). Endosome-associated complex, ESCRT-II, recruits transport machinery for protein sorting at the multivesicular body. *Developmental Cell, 3*, 283-289.

Bsbst, M., Katzmann, D., Estepa-Sabal, E., Meerloo, T., & Emr, S. (2002). ESCRT-III: an endosome-associated heterooligomeric protein complex required for MVB sorting. *Developmental Cell, 3*, 271-282.

Butterfield, D. (2002). Amyloid beta-peptide(1-42)-induced oxidative stress and neurotoxicity: implications for neurodegeneration in Alzheimer's disease brain. *Free Radical Research, 36*, 305-313.

Chiron, N., & Michelot, D. (2005). Odeurs de champignons: chimie et rôle dans les interactions biotiques — une revue. *Cryptogamie Mycologie, 26*, 299-364.

Chowienczyk, P. B.-J. (2000). Oral treatement with an antioxidant (raxofelast) reduces oxidative stress and improves endothelial function in men with type II diabetes. *Diabetologia, 43*, 973-977.

Cilek, J., & Hallmon, C. (2008). Controlled release chamber for dispensing aromatic substances. *Journal of the American Mosquito Control Association, 24*, 594-597.

Cole R & Schweikert M. (2003). *Handbook of Secondary Fungal Metabolites* (Vols. 1-3). Amsterdam: Academic Press.

Combet, E., Henderson, J., Eastwood, D., & Burton, K. (2006). Eight-carbon volatiles in mushrooms and fungi: properties, analysis, and biosynthesis. *Mycoscience, 6*, 317-326.

Coux, O., Tanaka, K., & Goldberg, A. (1996). Structure and functions of the 20S and 26S proteasomes. *Annual Review of Biochemistry, 65*, 801-847.

Dolinski, K., & Botstein, D. (2007). Orthology and functional conservation in eukaryotes. *Annual Review of Genetics, 41*, 465–507.

Eruslanov, E. K. (2010). Identification of ROS using oxidized DCFDA and flow-cytometry. *Methods in Molecular Biology, 594*, 57-72.

Giaever, G. (2002). Functional profiling of the *Saccharomyces cerevisiae* genome. *Nature, 418*, 387-391.

Gottesman, S., & Maurizi, M. (1992). Regulation by proteolysis: energy-dependent proteases and their targets. *Microbiol Review, 56*, 592-621.

Grant, C. M. (1997). Mitochondrial function is required for resistance to oxidative stress in the yeast Saccharomyces cerevisiae. *FEVS Letters, 410*, 219-222.

Hagen, T. H. (1994). Extensive oxidative DNA damage in hepatocytes of transgenic mice with chroinc active hepatitis destined to develop hepatocellular carcinoma. *PNAS, 91*, 12808-12812.

Halliwell, B. (2001). Role of free radicals in the neurodegenerative diseases: therapeutic implications for antioxidant treatment. *Drugs Aging, 18*, 685-716.

Henne, W., Buchkovich, N., & Emr, S. (2011). The ESCRT Pathway. *Developpmental Cell, 21*, 77-91.

Hershko, A., & Ciechanover, A. (1998). The ubiquitin system. *Annual Review of Biochemistry*, 425-479.

Hochstrasser, M. (1996). Ubiquitin-dependent protein degradation. *Annual Review of Genetics, 30*, 405-439.

Inamdar, A., Masurekar, P., & Bennett, J. (2010). Neurotoxicity of fungal volatile organic compounds in *Drosophila melanogaster. Toxicological Sciences, 117*, 418-426.

Inamdar, A., Moore, J., Cohen, R., & Bennett, J. (2012). A model to evaluate the cytotoxicity of the fungal volatile organic compound 1-octen-3-ol in human embryonic stem cells. *Mycopathologia, 173*, 13-20.

Kaminski, E., & Wasowicz, E. (1974). Volatile flavor compounds produced by molds of Aspergillus, Penicillium, and Fungi imperfecti. *Applied Microbiology, 27*, 1001-1004.

Katzmann, D., Babst, M., & Emr, S. (2001). Ubiquitin-dependent sorting into the multivescular body pathway requires the function of a conserved endosomal protein sorting complex, ESCRT-I. *Cell, 106*, 145-155.

Kimura, Y., & Tanaka, A. (2009). An inhibitor of a deubiqitinating enzyme regulates ubiquitin homeostasis. *Cell, 137*, 549-559.

Kimura, Y., & Tanaka, K. (2010). Regulatory mechansisms involved in the control of ubiquitin homeostasis. *Journal of Biochemistry, 147*, 793-798.

Li, W., Bengtson, M., & Ulbrich, A. (2008). Genome-Wide and functional annotation of human E3 ubiquitin ligases identifies MULAN, a mitochondrial E3 that regulates the organelle's dynamics and signaling. *PLoS One, 3*, e1487.

Lin, Y., Kuo, J., & M, J. (2007). Interactions between U-937 human macrophages and cationic dendrimers. *Journal of Controlled Release, 120*, 51-59.

Luhtala, N., & Odorizzi, G. (2004). Bro1 coordinates deubiquitination in the multivesicular body pathyway by recruiting Doa4 to endosomes. *The Journal of Cell Biology, 166*, 717-729.

Mukhopahyay, D., & Riezman, H. (2007). Proteasome-idenpendent functions of ubiquitin in endocytosis and signaling. *Science, 315*, 201-205.

Papa, F., & Hochstrasser, M. (1993). The yeast DOA4 gene encodes a deubiquitinating enzyme related to a product of the human tre-2 oncogene. *Nature, 10*, 313-319.

Papa, F., Amerik, A., & Hochstrasser, M. (1999). Interaction of the Doa4 deubiquitinating enzyme with the yeast 26S proteasome. *Molecular Biology of the Cell*, 741-756.

Parthasarathy, S. S. (2000). Potential role of oxidized lipids and lipoproteins in antioxidant defense. *Free Radical Research, 33*, 197-215.

Pickart, C. (1997). Targeting of substrates to the 26S proteasome. *Molecular Biology of the Cell, 11*, 1055-1066.

Pommerville, J. C. (2009). *Alcamo's Fundamentals of Microbiology.* Sudbury: Jones & Bartlett Publishers.

Raymond, C., Howald-Stevenson, I., Vater, C., & Stevens, T. (1992). Morphological classification of the yeast vacuolar protein sorting mutants: evidence for a prevacuolar compartment in class E vsp mutants. *Molecular Biology of the Cell, 3*, 1389-1402.

SGD Project. (n.d.). *SGD Gene Nomenclature Conventions*. Retrieved December 7, 2011, from Saccharomyces Genome Database: http://www.yeastgenome.org/help/yeastGeneNomenclature.shtml

SGD Project. (n.d.). *SGD Gene Ontology Slim Mapper*. Retrieved Feb 07, 2011, from Saccharomyces Genome Database: http://www.yeastgenome.org/cgi-bin/GO/goSlimMapper.pl

Splivallo, R. (2007). Truffle volatitles inhibit growth and induce an oxidative burst in Arabidopsis thaliana. *New Phytol, 175*, 417-424.

Sullivan, P., Dragicevic, N., Deng, J., Bai, Y., Dimayuga, E., Ding, Q., et al. (2004). Proteasome inhibition alters neuroal mitochondrial homeostasis and mitochodria turnover. *Journal of Biological Chemistry, 279*, 20699-20707.

Thermo Scientific. (n.d.). *Yeast Knockout Strains*. Retrieved Feburary 18, 2012, from Open Biosystems RNAi, Gene Expression, Antibodies: https://www.openbiosystems.com/GeneExpression/Yeast/YKO/

Varshavsky, A. (1997). The ubiquitin system. *Trends Biochem Sci., 67*, 383-387.

Wach, A. B. (1994). New heterologous modules for classical or PCR-based gene disruptions in Saccharomyces cerevisiae. *Yeast, 10*, 1793-1808.

Wilkins, K., & Larsen, K. (1995). Variation of volatile organic compound patterns of mold species from damp buildings. *Chemosphere, 31*, 3225-3236.

Wolfe, D., Reiner, T. K., Pizzini, M., & Keil, R. (1999). Ubiquitin metaolism affects cellular response to volatile anesthetics in yeast. *Molecular and Cellular Biology, 19*, 8254-8262.